Northumbria Research Link

Tapered microfiber MZI Biosensor for highly sensitive detection of *Staphylococcus aureus*

Hou-Chang Li[#], Yuan-Kui Leng[#], Yun-Cheng Liao[#], Bin Liu[*], Wei Luo, Juan Liu, Jiu-Lin Shi, Jinhui Yuan[*], Heng-Yi Xu, Yong-Hua Xiong, Xing-Dao He and Qiang Wu[*]

Abstract—A new double-taper microfiber Mach-Zehnder interferometer (MZI) biosensor is applied for *Staphylococcus aureus* (*S. aureus*) detection. The microfiber MZI structure is fabricated by creating two tapers along a traditional single mode fiber (SMF) firstly and tapering the SMF sandwiched between two tapers into very small diameter (in the order of micrometers). The measured refractive index (RI) sensitivity of the microfiber MZI is up to 2731.1 nm/RIU in the RI range of 1.34 when the taper waist diameter was 10.2 µm, which is in good agreement with numerical simulation results by using the beam propagation method (BPM). The microfiber MZI functionalized with pig immunoglobulin (pig IgG) could be used to specifically binding to *S. aureus*. In experiment, the maximum wavelength shift of 1.408 nm was achieved when the microfiber biosensors were immersed into *S. aureus* with concentration of 7×10^1 CFU/mL. The limit of detection (LoD) of the microfiber biosensor for *S. aureus* is calculated as low as 11 CFU/mL. The proposed microfiber MZI biosensor has advantages of simple structure configuration, high sensitivity, good repeatability and specificity, wide detection range and fast detection response time (<30 minutes) and thus was demonstrated a good application prospect in food safety inspection, biochemical sensing, diseases and medical diagnostics.

Index Terms—Optical fiber sensor, biosensor, Mach-Zehnder interferometer (MZI), *Staphylococcus aureus* (*S. aureus*)

I. Introduction

S*taphylococcus aureus* (*S. aureus*) which was discovered by Dr. Alexander ogston is a gram-positive spherical bacteria. It is widely present in the natural environment and can produce enterotoxins under appropriate conditions, leading to food poisoning [1-3]. Recently, numerous reports about food poisoning caused by *S. aureus*, it accounts for a quarter of food-borne microbial food poisoning events, second only to *Salmonella* and *parahaemolyticus* [4]. Therefore, the detection of food-borne pathogens and the reduction of the incidence of food-borne diseases have always received much attention [5]. Some conventional detecting techniques of foodborne pathogens, including polymerase chain reaction (PCR), enzyme-linked immunosorbent assay (ELISA) method and so

on, have good reliability, but time-consuming, typically requiring 24-48 hours to grow bacteria on plates in enriched media, which cannot meet the convenient and fast analysis of detecting foodborne pathogens [6]. In order to solve this problem, many new rapid, sensitive and specific diagnostic methods have been proposed in recent years [7-9]. Among these methods, fiber-based biosensor is a label-free technique, which needs to deposit antigen/antibody on the surface of optical fiber sensors acting as "capture" elements to specific binding to biomolecules. By detecting the optical signal variation, the concentration of the analyte will be determined once the sensor is calibrated. Compared with the traditional methods, such as PCR and ELISA, the optical fiber-based immunological sensor method has the advantages of high sensitivity, simple operation, and monitored real-time and thus has become a hot research topic. According to different working principles, the main types of optical fiber biosensors include optical fiber interferometer [10,11], fiber surface plasmon resonance [12,13], fiber grating [14,15], and whispering-gallery-mode resonator [16,17]. Among them, the interferometer biosensor is widely concerned due to the advantages of high sensitivity, low cost, and simple fabrication. A microfiber is the collective name of fiber with a diameter of micron or nanometer, which can excite a strong evanescent field and thus is an ideal candidate for biosensing application. On the other hand, a microfiber interferometer produces significant coherent peak or coherent valley spectra, which can be used to monitor wavelength shift (peak or dip) with unique advantage of independent to power variation of optical source, providing better measurement accuracy compared to monitoring power of the sensor. The microfiber interferometer biosensor is currently the hot research topic over the world.

Hou-Chang Li, Yun-Cheng Liao, Bin Liu, Wei Luo, Juan Liu, Jiu-Lin Shi, Xing-Dao He and Qiang Wu are with Key Laboratory of Opto-Electronic Information Science and Technology of Jiangxi Province, Nanchang Hangkong University, Nanchang 330063, China (e-mail: lihouchang104@163.com; yunchengl@126.com; liubin_d@126.com; 15292080721@163.com; 18042@nchu.edu.cn; jiulinshi@126.com; hxd@nchu.edu.cn; qiang.wu@northumbria.ac.uk). Qiang Wu is also with Faculty of Engineering and Environment, Northumbria University, Newcastle Upon Tyne NE1 8ST, UK.

Yuan-Kui Leng, Heng-Yi Xu and Yong-Hua Xiong are with State Key Lab Food Sci & Technol, Nanchang University, Nanchang, Peoples R China. (e-mail: yuankuilengxq@163.com; HengyiXu@ncu.edu.cn; yhxiongchen@163.com).

Jinhui Yuan are with the Research Center for Convergence Networks and Ubiquitous Services, University of Science & Technology Beijing, Beijing 100083, China. (e-mail: yuanjinhui81@163.com).

According to different optical path principles, the microfiber interferometers can be divided into: multimode interferometer [18-22], Sagnac based microfiber interferometer [23,25] and Mach-Zehnder interferometer (MZI) [26-28]. Compared with other microfiber sensor structures, the fiber diameter of the microfiber interferometer can be made relatively large, less affected by environmental instability factors, and its sensitivity is higher. Salceda-Delgado G *et al* fused a tapered fiber with a diameter of 10 μm to two ordinary single-mode fibers (SMFs), and extracted the spatial light frequency by performing a Fourier transform of the transmission spectrum to achieve temperature-insensitive refractive index (RI) sensing with a resolution of up to 3.7×10^{-6} [29]. Liu *et al* used fusion taper technology to taper the SMS (single-mode-multimode-single-mode) fiber structure to between 10-20 μm. It is also used for RI sensing with a sensitivity of 19212.5 nm/RIU [30].

In recent years, people have used optical fiber sensors to carry out research in the detection of foodborne pathogens. For example, *Zibaii et al* used a tapered fiber to directly detect the growth process of *E. coli K-12* [31]. T. Liu *et al.* applied propidium iodide to the end of the tapered fiber to detect dead *E. coli*, and its LoD value was 10^4 cells/mL [32]. Y. Li *et al.* proposed and demonstrated a phage-based fast-response multimode microfiber probe (S = 2178 nm/RIU) to detect *E. coli*, with a LoD value of 10^3 CFU/mL [33]. K. Dandapat *et al.* used the maximum RI sensor (S = 1929 nm/RIU) obtained by the response wavelength conversion point of the long-period grating to detect *E. coli*, and its LoD value was 10^2 CFU/mL [34]. Ling Chen *et al* proposed a tapered singlemode-no core-singlemode fiber coupler structure (S = 1523 nm/RIU) for *S. aureus* detection [35]. However, those above methods have its disadvantages such as low sensitivity and complicated fabrication and so on.
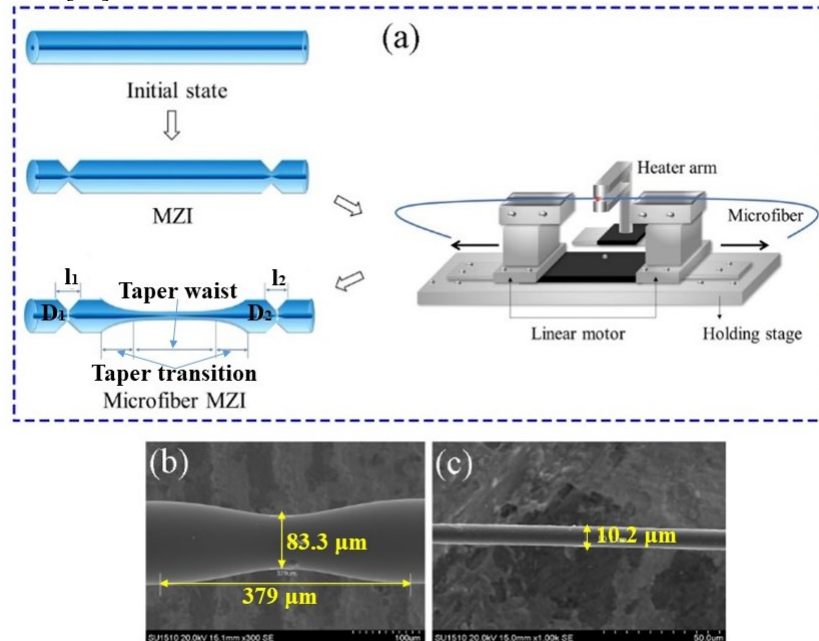

Fig. 1. (a) Sensor preparation process diagram; (b) SEM image of one of the MZI arms; (c) SEM image of taper waist.

In this paper, we propose a new microfiber MZI biosensor with simple configuration where a SMF sandwiched between two tapers was tapered into microfiber with diameters in the order of ten micrometers. The characteristics of the sensor and the spectral response of RI are studied by employing the beam propagation method (BPM). The effect of waist diameter on surrounding RI sensing responses is experimentally analyzed in detail. Then, the double taper microfiber MZI was functionalized with Pig IgG, sensitivity and specificity for detection of *S. aureus* are tested and analyzed based on the microfiber MZI biosensors. When the concentration of S. aureus was as low as 7×10^1 CFU/mL, the wavelength shift of the double taper microfiber MZI biosensor was 1.408 nm.

II. STRUCTURE CONFIGURATION AND NUMERICAL SIMULATION

The microfiber MZI structure is composed of two tapers (non-adiabatic) and microfiber (adiabatic) sandwiched between the two tapers as shown in Figure 1(a). The two tapers are equivalent to the beam splitter and coupler. When the light travels through the first taper, the mode field mismatch of the single-mode fiber will excite the cladding modes, which will travel along the microfiber and then re-couples to the core mode of SMF through the second taper. In the output of SMF, due to the phase difference between the core mode and the cladding modes within the microfiber, MZI interference was take place and different interference light intensities are generated.

In our previous work, a double-taper fiber MZI structure was fabricated by using arc discharge of a traditional fusion splicer (Fujikura 80c) [36]. The discharge time and power of the fusion splicer was set to 2000 ms and 100 bits, respectively. However, the fiber MZI is insensitive to the change of surrounding RI. So, it was then tapered by the Commercial Optical Coupler Manufacturing System (OC-2010, JILONG) into microfiber with taper waist diameter in the order of ten micrometers in order to achieve a highly sensitive refractive index response. The typical structural parameters of tapered microfiber MZI were obtained with SEM in Figs. 1(b) and (c). $l_1 = l_2$, $D_1 = D_2$

and taper waist of microfiber are 379, 83.3 and 10.2 μm, respectively.

The beam propagating method (BPM) was used for the numerically study the light transmission of the proposed double taper microfiber MZI. Under the condition of slowly varying envelope approximation, it can be derived from Maxwell's equations:

$$2j\beta \frac{\partial \varphi}{\partial z} = \frac{\partial^2 \varphi}{\partial x^2} + \frac{\partial^2 \varphi}{\partial y^2} + k_0^2(n^2 - n_{eff}^2)\varphi \qquad (1)$$

Among them: φ is the envelope function of the field; β is the propagation constant; k_0 is the wave-number; n_{eff} is the effective RI. Use uniformly distributed calculation grid sizes in the x and z directions of the 2D model, the grid sizes are set as 0.1 μm and 1 μm along X and Z directions, respectively. The boundary condition used in the model is perfectly matched layer (PML) condition. Standard Corning SMF with 125 μm diameter cladding, 8.2 μm diameter core, and the corresponding RIs are 1.4507 and 1.4428, respectively, are used for the construction of the model. The length of the taper $l_1 = l_2$ and the taper diameter ($D_1 = D_2$) were set to 400 and 80 μm, respectively. And the diameter and length of taper waist were set to 10 μm and 12 mm, respectively. The spectral responses at surrounding RI range of 1.34 were simulated numerically as shown in Fig. 2(a), and a linear RI sensitivity of 2891 nm/RIU was achieved [Fig. 2(b)]. The optical field distribution along the microfiber MZI at 1538.0 nm (dip) and 1539.9 nm (peak) is shown in Figs. 2(c) and (d).
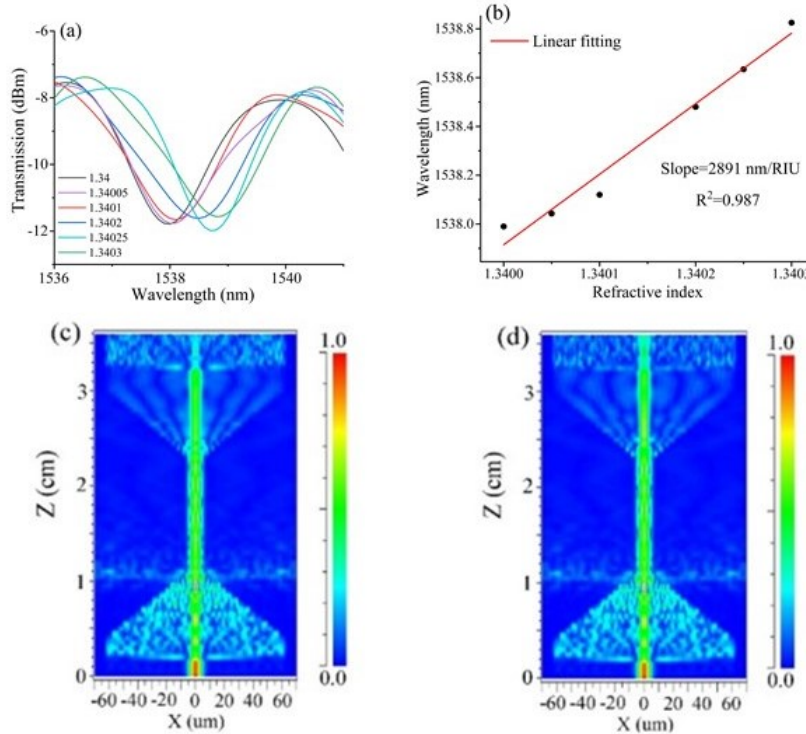

Fig. 2. (a) Simulated spectral response of a taper microfiber MZI with a microfiber length set to 12 mm and a 7 mm tapered transition zone in the RI range of 1.34; (b) calculated RI sensitivity at RI range of 1.34; (c) and (d) The distributions of optical field and normalized optical intensity propagating along microfiber MZI at 1538.0 nm (dip) and 1539.9nm (peak).

III. EXPERIMENTAL RESULTS AND DISCUSSION

A. RI sensitivity

RI sensitivity of the proposed double taper microfiber MZI sensor was firstly investigated by preparing three microfiber MZIs with taper diameters of 58, 30 and 10.2 μm, which were recorded as S-1, S-2, and S-3, respectively. Figure 3(a)-(c) shows the measured spectral responses of surrounding RI, and the wavelength shifts of the three sensors vs. RI were summarized in Fig. 3(d). When the RI increases in the range of 1.34, the transmission dips of all the three sensors have obvious redshift. As the taper waist diameter decreases from 58 to 10.2 μm, the RI sensitivity of the microfiber MZI increases significantly. The RI sensitivities of the three sensors are 460.0, 1333.0 and 2731.1 nm/RIU corresponding to S-1, S-2, and S-3, respectively. In addition, the RI sensitivity of the selected biosensor S-3 in the RI range of 1.373-1377 and 1.410-1.414 is 5182.0 and 12221 nm/RIU, respectively. The measured sensitivity with about 10 μm taper diameter almost identical with simulations as a result (2865 nm/RIU). The results show that as the diameter of the taper waist of the sensor decreases, the sensitivity of the RI of the biosensor increases significantly. The measured sensitivity of S-3 (with 10.2 μm taper waist diameter) agrees very well with the simulated result (2865 nm/RIU). In addition, studies have shown that considering the turning point of microfiber dispersion, the sensitivity of the sensor to environmental index changes can be further improved, and near the turning point (fiber diameter is 4.6 μm) to achieve ultra-high sensitivity of 10777.8 nm/RIU [37]. However, there is a trade-off between the sensitivity and stability for this type of sensor. Therefore, in our experiments the double taper microfiber MZI sensor with taper waist diameter of about 10 μm was used for biological sensing study.

The temperature dependance of the sensor within 20-48 °C is shown in Figures 4 (a) and (b), and the temperature sensitivity is -0.031 nm/°C. This suggests the temperature has a limited influence on measurement accuracy (our biological

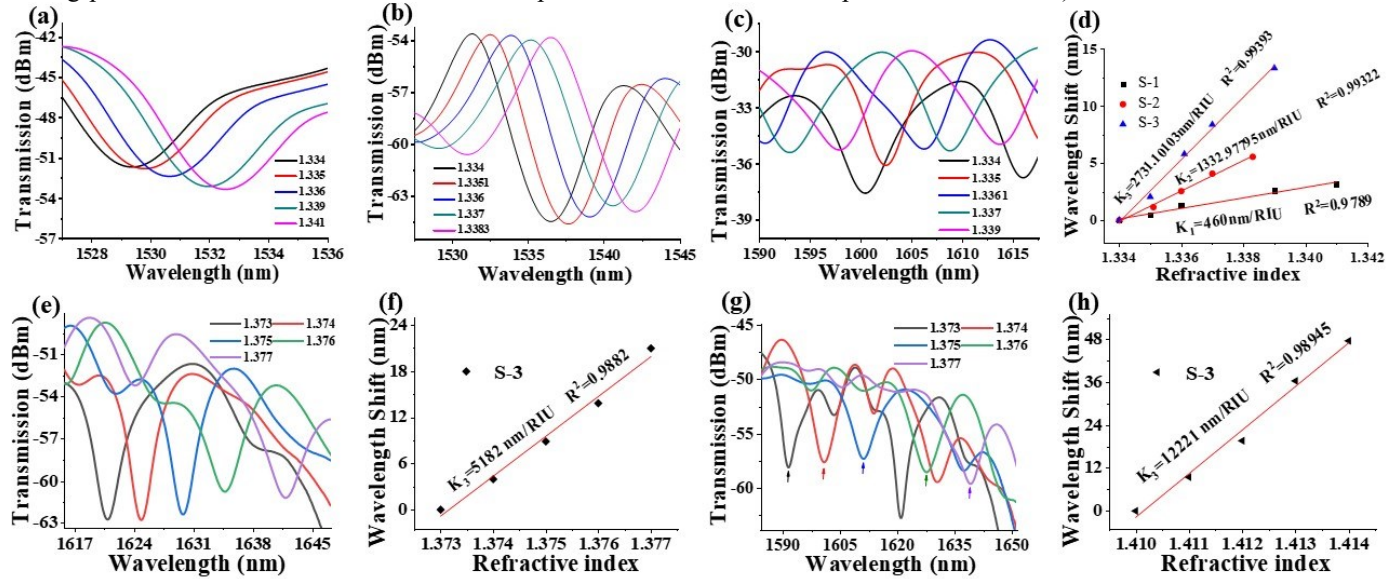testing processes are all carried out at room temperature with
narrow temperature fluctuations).

Fig. 3. Sensor wavelength shift spectrum of different taper waist diameters (a) 58 μm; (b) 30 μm; and (c) 10.2 μm. (d) The change of the center wavelength of the transmission spectrum with RI. (e)-(h) Spectral drift and corresponding sensitivity of S-3 in different refractive index ranges.
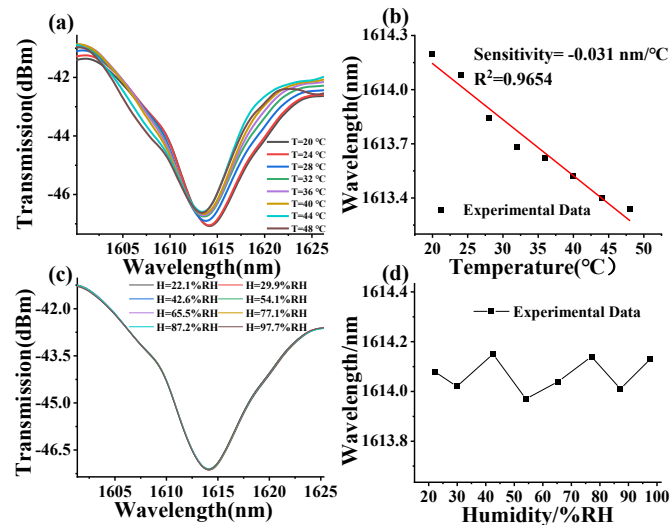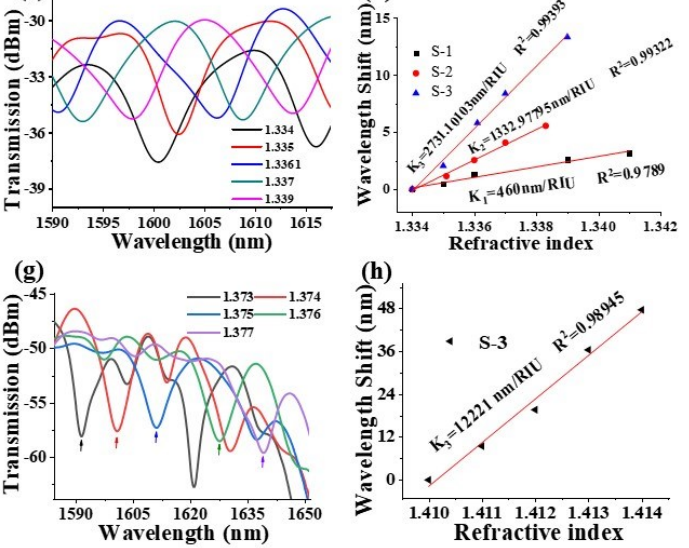

Fig. 4. (a) and (b) The temperature sensitivity of the sensor; (c) and (d) The humidity sensitivity of the sensor.

B. Sensor functionalization

To utilize the double taper microfiber MZI sensor for *S. aureus* detection, functionalization of Pig IgG antibody on surface of the microfiber is required, which will specifically binding to *S. aureus*. The process of sensors functionalization is described below and illustrated in Fig. 5:

(a) Firstly, the optical fiber surface was cleaned by treating with 5% KOH standard solution for 1 hour. In order to immobilize the pig IgG antibody onto fiber surface, the optical fiber is required to be activated first. The silica optical fiber surface contains a large amount of silanol. By immersing the optical fiber into a 5% silanized ethanol solution for 4 hours, the silane agent in the acid anhydride will hydrolyze to carboxyl groups. Figures 6(a) and (b) show the SEM of mass spectrometry analysis image

measured by field emission scanning electron microscope (FESEM) and elemental composition after silanization.

(b) The sensor was then immersed into EDC solution (1-(3-Dimethylaminopropyl)-3-ethylcar-bodiimide hydrochloride) in PBS buffer about 30 min; and then immediately by dipping in the mixed solution of EDC and NHSS (hydroxy-2,5-dioxopyrolidine-3-sulfonicacid sodium salt) about 30 min to activate the surface carboxyl group (generate active fat).

(c) After washing several times with deionized water, the fibers were dispersed in pig IgG in PBS solution with the concentration of 50 ug/mL. The sensor was connected to an OSA (AQ6370) for real-time monitoring the immobilization of Pig IgG [Figs. 7(a) and (b)]. It is possible to see that the spectral shift tends to be stable until about 100 mins, indicating that the immobilization of Pig IgG antibody has been saturated. Then, the fiber surface was washed with deionized water to remove non-bind Pig IgG.

(d) After washing with deionized water, the sensor was immersed in bovine serum albumin (BSA) for 1 hour to block the remaining carboxyl groups not binding to Pig IgG antibody, which will prevent nonspecific bind in the following measurements. Sensor surface was washed with deionized water.

(e) The above-functionalized microfiber biosensor was immersed into the *S. aureus* solution to monitor the real time binding process between Pig IgG antibody and *S. aureus*. Figures 6(c) and (d) show the FESEM image and mass spectrometry analysis image of pig IgG bind with *S. aureus*, respectively. The above characterizations reveal that the *S. aureus* was effectively captured on the microfiber surface.
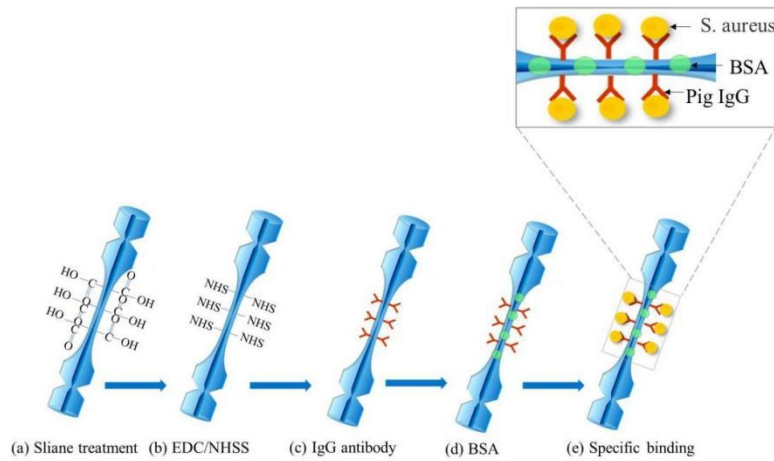
Fig. 5. Schematic diagram of biological modification process (a) sensor after silanization; (b) sensor after EDC / NHSS activation; (c) sensor after antibody modification; (d) blocking remaining carboxyl groups by BSA; (e) antibody antigen Combining process.
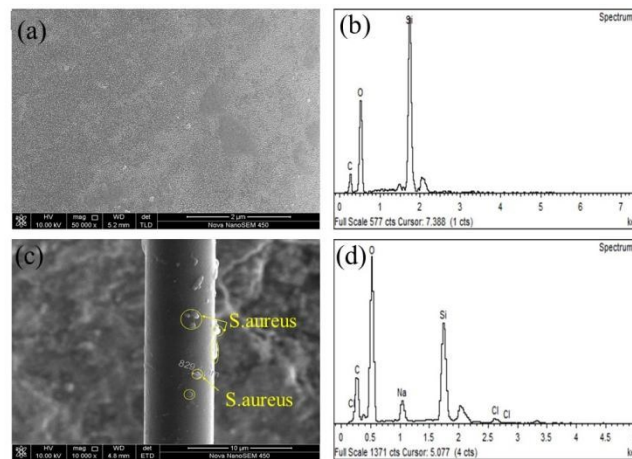
Fig. 6. (a) FESEM photo of the silanized fiber surface; (b) Mass spectrometry analysis image on the surface of the optical fiber after silicidation; (c) FESEM photo of antibody Pig IgG binding to *S. aureus*; (d) mass spectrometry analysis image on the surface of the optical fiber after the antibody porcine IgG is combined with *S. aureus*.
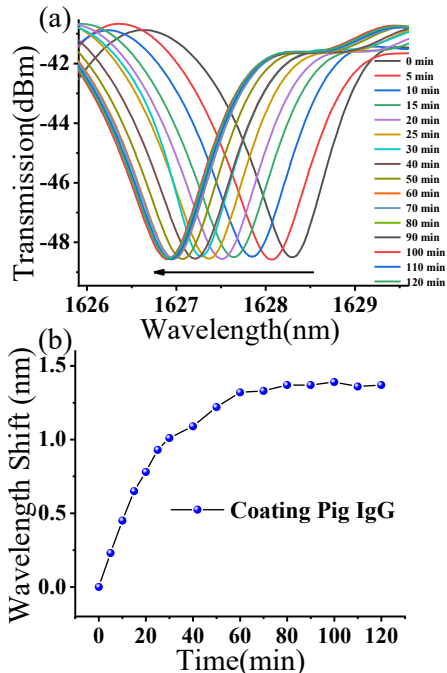
Fig. 7. (a) and (b)Wavelength shift of the biosensor spectra during the process of modifying the fiber surface by immobilization of pig IgG over it.

C. Results and discussion

The detection of *S. aureus* is shown in Figure 8. The microfiber MZI sensor was connected to the BBS (SC-5-FC) and OSA for recording the spectral response of the developed biosensor at different concentrations of *S. aureus*. The volume of *S. aureus* solutions was about 2000 μL per experiment.

Fig. 8. Schematic diagram of the experimental device.

The functionalized microfiber MZI biosensor was firstly immersed into PBS buffer for 20 minutes to test the stability of the biosensor. The maximum wavelength variations are not more than ±0.02 nm over 20 min in the PBS [Fig. 9(a)]. The

fiber biosensor was then immersed into different concentrations (from low to high, 7×10^1, 7×10^2, 7×10^3, 7×10^4, and 7×10^5 CFU/mL) of *S. aureus* solution for about 40 minutes each time. Before testing different concentrations of *S. aureus* solution, the biosensor needs to be immersed in PBS buffer for washing the nonspecific bind between IgG antibody and *S. aureus*. During the process, the pig IgG on the surface of microfiber MZI will specifically capture *S. aureus*, resulting in the physical property changes to the fiber biosensor (effective diameter, RI) and thus introduce changes in the transmission spectrum. Figure 9(b) shows spectral responses with time, when a mi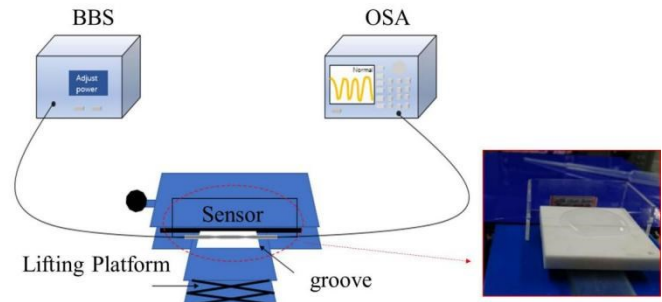crofiber MZI biosensor (functionalized with 50 µg/mL pig IgG) was immersed into *S. aureus* solution with a concentration of 7×10^1 CFU/mL. The wavelength change mainly occurs in the first 20 minutes, which is much larger than the movement amount of the last 20 minutes and tends to be stable. This result is consistent with the kinetics of the biological reaction law.
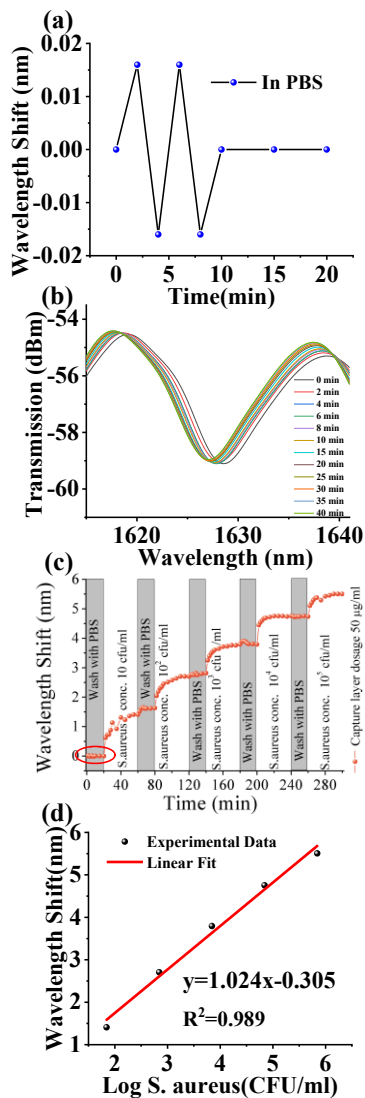

Fig. 9. (a) Wavelength shift response when no biological binding occurs in PBS solution; (b) spectral response of biosensor functionalized with 50 µg/mL antibody pig IgG, used to detect *S. aureus* at a concentration of 7×10^1 CFU/mL; (c) wavelength shift vs. time in different concentrations of *S. aureus*. (d) Calibration curve for S. aureus with a concentration range of 10^1-10^5 CFU/mL.

Before changing the *S. aureus* solution with higher concentration, the fiber biosensor was immersed into PBS buffer for about 20 minutes for washing out nonspecific bind with *S. aureus*. The wavelength shifts of the microfiber MZI biosensor (functionalized with 50 µg/mL pig IgG solution) over time was shown in Fig. 9(c), indicating the dynamic binding between IgG antibody and *S. aureus*. It is noted that the wavelength shift is very small (less than 0.02 nm) in the PBS buffer solution, which indicate that the nonspecific bind with *S. aureus* is neglectable. When the concentration of the *S. aureus* solution is 7×10^1 CFU/mL, the wavelength shift due to the bind between pig IgG and *S. aureus* is 1.408 nm. The wavelength shifts are 2.704 nm, 3.792 nm, 4.752 nm, and 5.504 nm corresponding to *S. aureus* concentration of 7×10^2, 7×10^3, 7×10^4 and 7×10^5 CFU/mL, respectively. This result shows that the developed double taper microfiber MZI biosensor can detect the concentration of *S. aureus* effectively. In biosensing, LoD represents the lowest detectable concentration of the analyte in the sample (LoD = 3.3 standard deviation of blank samples(σ) / slope of the calibration line). The results show that the calibration curve shows a good the linearity (correlation coefficient is 0.989 [Fig. 9(d)]). The remaining standard deviation of the regression line was used as the standard deviation of blank samples (σ = 0.3255) and the LoD of the sensor was calculated to be 11 CFU/mL.

In addition, we also conducted a reproducibility test by fabricating five biosensor samples (same manufacturing parameters, modified antibody pig IgG concentration) to perform multiple tests on the same concentration of *S. aureus*. The results [Fig. 10(a)] clearly verified that the proposed sensor indicating excellent reproducibility. The binding specificity of the fiber sensor was studied by immersing it into *E. coli*, BSA and human chorionic gonadotropin (hCG) solutions, and the measured wavelength shifts were 0.16, 0.22 and 0.42 nm respectively [shown in Fig. 10(b)], which were much smaller than that in *S. aureus* solution (shift 5.88 nm). The results demonstrated a good selectivity and specificity in detecting *S. aureus*.
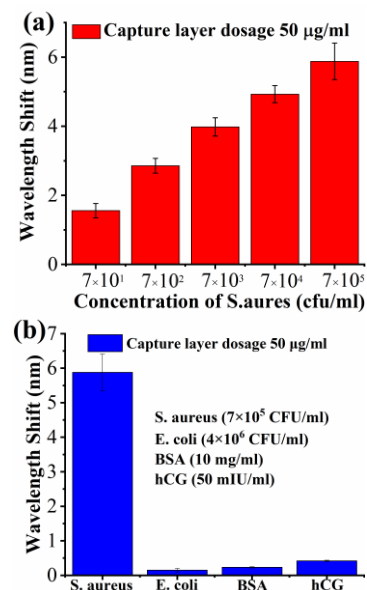

Fig. 10. (a) Reproducibility: wavelength shift vs. concentration of *S. aureus* and (b) specificity results of the biosensor.

The advantages of our proposed biosensor compared with others pathogenic bacteria biosensor are shown in Table 1. Method performances allow analytes to be detected as low as 11 CFU/mL (LoD). This is one of the best results reported to date, these tests have shown superior performance of this sensor.

TABLE 1
Comparison of the analysis characteristics of the immunosensor developed in this research and related immunosensors.

Transducer	Pathogenic bacteria	dynamic range (CFU/ml)	response time (min)	LOD	Ref.
Dual-color upconversion fluorescence and magnetic nanoparticles	*S. aureus*	10^1-10^5	60	8 CFU/mL	[38] (2012)
Magnetic beads (MBs) and gold screen-printed electrodes (Au/SPEs)	*S. aureus*	1–10^7	120	1 CFU/mL	[39] (2012)
Surface plasmon resonance (SPR)	*S. aureus*	-	20	10 CFU/mL	[40] (2013)
Gold nanoparticle	*S. aureus*	10-10^6	240	9 CFU/mL	[41] (2014)
Chemically modified graphene	*S. aureus*	-	1-2	1 CFU/mL	[42] (2014)
Magnetically assisted surface-enhanced Raman scattering (SERS)	*S. aureus*	10-10^5	-	10 cells/mL	[43] (2015)
Dual-aptamer-based sandwich immunosensor	*S. aureus*	10-10^6	-	1 CFU/mL	[44] (2015)
Microdisks whispering gallery mode (WGM)	*S. aureus*	5×10^6-5×10^9	30	5 pg/mL	[45] (2016)
Magnetic nanobeads and gold surface	*S. aureus*	7.5-7.5×10^6	-	7-100 CFU/mL	[46] (2016)
Long-period fiber gratings (LPFGs)	*S. aureus*	10^4-10^8	30	224 CFU/mL	[47] (2019)
Fluorescent (optical) bioprobe	*S. aureus*	40×10^2-4×10^8	20	85 CFU/mL	[48] (2019)
Double-taper microfiber Mach-Zehnder interferometer (MZI)	*S. aureus*	7×10^1-7×10^5	20	11 CFU/mL	this paper

IV. CONCLUSION

A new highly sensitive microfiber MZI biosensor was proposed and experimentally demonstrated for application to *S. aureus* detection. The proposed microfiber MZI structure consists of two tapers and SMF, which are tapered to small diameter. When the taper diameter is 10.2 μm, the RI sensitivity of the microfiber MZI is as high as 2731.1 nm/RIU within the RI range of 1.34, which meets well with numerical simulation by using BPM. The surface of the microfiber MZI was functionalized with pig IgG for specifically capturing *S. aureus*. The experimental results show that a detection concentration limit (7×10^1 CFU/mL) of the biconical micro-fiber MZI biosensor can be achieved, and the excellent LoD can reach as low as 11 CFU/mL. Furthermore, the sensor has a high detection range (from 7×10^1 to 7×10^5 CFU/mL) and rapid detection response time (less than 30 minutes). In addition, a good reproducibility and specificity for the optical fiber sensor have been demonstrated experimentally. Therefore, the proposed sensor has a good application prospect in biomedicine, biochemical pollution, food safety and others fields.

REFERENCES

[1] D.D. Pang, Q.M. Sui, "A relocatable resonant FBG-acoustic emission sensor with strain-insensitive structure," Optoelectronics Letters, vol. 10, no. 2, pp. 96-99, 2014.

[2] A. Ogston, "On Abscesses," Clinical Infectious Diseases, vol. 6, no. 1, pp. 122-128, 1984.

[3] http://www.cdc.gov/foodborneburden/2011-foodborne-esti mates.html.

[4] G.A. Suaifan, S. Alhogail, M. Zourob, "Rapid and low-cost biosensor for the detection of Staphylococcus aureus," biosensors & bioelectronics, vol. 90, pp. 230-237, 2017.

[5] P. Elizabeth, "Community-acquired methicillin-resistant Staphylococcus aureus infections," Clinics in Laboratory Medicine, vol. 24, no. 2, pp. 403-418, 2004.

[6] K. Yamada, W. Choi, I. Lee, and S. Jun, "Rapid detection of multiple foodborne pathogens using a nanoparticle-functionalized multi-junction biosensor," Biosensors and Bioelectronics, vol. 77, no. 15, pp. 137-143, 2016.

[7] X. Zhao, C.W. Lin, and J. Wang, "Advances in Rapid Detection Methods for Foodborne Pathogens," Journal of Microbiology and Biotechnology, vol. 24, no. 3, pp. 297-312, 2014.

[8] M.L. Bhaisare, G. Gedda, and M.S. Khan, "Fluorimetric detection of pathogenic bacteria using Magnetic carbon dots," Analytica Chimica Acta, vol. 920, no. 12, pp. 63-71, 2016.

[9] W.F. Law, N.S. Mutalib, and K.G. Chan, "Rapid methods for the detection of foodborne bacterial pathogens: principles, applications, advantages and limitations," Frontiers in Microbiology, vol. 5, no. 6, pp. 770-789, 2015.

[10] Y. Zhao, J. Zhao, and Q. Zhao, "Review of No-core Optical Fiber Sensor and Applications," Sensors and Actuators A Physical, vol. 313, pp. 112160, 2020.

[11] Y. Mustapha Kamil, M.H. Abu Bakar, and M.A. Mustapa, "Sensitive and Specific Protein Sensing Using Single-Mode Tapered Fiber Immobilized with Biorecognition Molecules," IEEE Photonics Journal, vol. 7, no. 6, pp. 1-9, 2015.

[12] R.L. Rich, D.G. Myszka, "Advances in Surface Plasmon Resonance Biosensor Analysis," Current Opinion in Biotechnology, vol. 11, no. 1, pp. 54-61, 2000.

[13] B.B. Luo, Y.J. Wang, H.F. Lu, S.X. Wu, Y. Lu, S.H. Shi, L.C. Li, S.H. Jiang, and M.F. Zhao, "Label-free and specific detection of soluble programmed death ligand-1 using a localized surface plasmon resonance biosensor based on excessively tilted fiber gratings," Biomed. Opt. Express, vol. 10, pp. 5136-5148, 2019.

[14] R. Srinivasan, S. Umesh, and S. Murali, "Bare fiber Bragg grating immunosensor for real-time detection of Escherichia coli bacteria," Journal of Biophotonics, vol. 10, no. 2, 2016.

[15] A. Juste-Dolz, M. Delgado-Pinar, and M. Avella-Oliver, "BIO bragg gratings on microfibers for label-free biosensing," Biosensors & Bioelectronics, vol. 176, pp. 112916, 2021.

[16] D. Yang, A. Wang, and J.H. Chen, "Real-time monitoring of hydrogel phase transition in an ultrahigh Q microbubble resonator," Photonics Research, vol. 8, no. 4, pp. 497-502, 2019.

[17] Y. Wang, H. Zhang, Y. Cui, W. Lin, B. Liu and D. Xiang, "Real-Time Conformational Change Monitoring of G-Quadruplex Using Capillary-Based Biocompatible Whispering Gallery Mode Microresonator," in IEEE Sensors Journal, vol. 20, no. 21, pp. 12558-12564, Nov. 2020.

[18] Q. Wu, Y. Semenova, and P. Wang, "High sensitivity SMS fiber structure based refractometer – analysis and experiment", Optics Express, vol. 19, no. 9, pp. 7937-7944, 2011.

[19] G. Salceda-Delgado, D. Monzon-Hernandez, A. Martinez-Rios, G.A. Cardenas-Sevilla, and J. Villatoro, "Optical microfiber mode interferometer for temperature-independent refractometric sensing," Optics Letters, vol. 37, no. 11, pp. 1974-1976, 2012.

[20] A.K. Mallik, "High sensitivity refractive index sensor based on a tapered small core single-mode fiber structure," Optics Letters, vol. 40, no. 17, pp. 4166-4169, 2015.

[21] A.A. Jasim, J. Faruki, M.F. Ismail, and H. Ahmad, "Fabrication and Characterization of Microbent Inline Microfiber Interferometer for Compact Temperature and Current Sensing Applications," Journal of Lightwave Technology, vol. 35, no. 11, pp. 2150-2155, 2017.

[22] Q. Wu, Y. W. Qu, J. Liu, J. H. Yuan, S. P. Wang, T. Wu, X. D. He, B. Liu, D. J. Liu, Y. Q. Ma, Y. Semenova, X. J. Xin, P. Wang and G. Farrell, "Singlemode-Multimode-Singlemode fibre Structures for Sensing Applications - A Review," IEEE Sensors Journal, vol. 21, no. 11, pp. 12734-12751, 2021.

[23] L. Sun, L. Jie, Y. Tan, S. Xiang, and B.O. Guan, "Miniature highly-birefringent microfiber loop with extremely-high refractive index sensitivity," Optics Express, vol. 20, no. 9, pp. 10180-10185, 2012.

[24] F. Wei, A.K. Mallik, D. Liu, W. Qiang, and Y. Semenova, "Magnetic field sensor based on a combination of a microfiber coupler covered with magnetic fluid and a Sagnac loop," Scientific Reports, vol. 7, no. 1, pp. 4725, 2017.

[25] S. Gao, L.P. Sun, L. Jie, L. Jin, and B.O. Guan, "High-sensitivity DNA biosensor based on microfiber Sagnac interferometer," Optics Express, vol. 25, no. 12, pp. 13305-13313, 2017.

[26] H. Luo, Q. Sun, Z. Xu, D. Liu, and Z. Lin, "Simultaneous measurement of refractive index and temperature using multimode microfiber-based dual Mach–Zehnder interferometer," Optics Letters, vol. 39, no. 13, pp. 4049-4052, 2014.

[27] N.J. Xie, H. Zhang, B. Liu, J.X. Wu, B.B. Song, and T.T. Han, "Highly sensitive in-line microfluidic sensor based on microfiber-assisted Mach–Zehnder interferometer for glucose sensing," Journal of Optics, vol. 19, pp. 115803, 2017.

[28] M.F. Jaddoaa, A.A. Jasimb, M.Z.A. Razakb, S.W. Harun, and H. Ahmad, "Highly responsive NaCl detector based on

inline microfiber Mach–Zehnder interferometer," Sensors and Actuators A: Physical, vol. 237, pp. 56-61, 2016.

[29] G. Salceda-Delgado, D. Monzon-Hernandez, and A. Martinez-Rios, "Optical microfiber mode interferometer for temperature-independent refractometric sensing," Optics Letters, vol. 37, no. 11, pp. 1974, 2012.

[30] D.J. Liu, A.K. Mallik, J.H. Yuan, C.X. Yu, G. Farrell, Y.Semenova, and Q. Wu, "High sensitivity refractive index sensor based on a tapered small core single-mode fiber structure," Optics Letters, vol. 40, no. 17, pp. 4166-4169, 2015.

[31] M.I. Zibaii, A. Kazemi, H. Latifi, M.K. Azar, S.M. Hosseini, and M.H. Ghezelaiagh, "Measuring bacterial growth by refractive index tapered fiber optic biosensor," Journal of Photochemistry and Photobiology B: Biology, vol. 101, pp. 313–320, 2010.

[32] T. Liu, Z. Yong, Z. Zhang, P. Zhang, J. Li, R. Yang, C. Yang, and Z. Lei, "A fiber optic biosensor for specific identification of dead Escherichia coli O157:H7," Sensors and Actuators B-Chemical, vol. 196, pp. 161–167, 2014.

[33] Y. Li, H. Ma, L. Gan, A. Gong, H. Zhang, D. Liu, and Q. Sun, "Immobilized optical fiber microprobe for selective and sensitive Escherichia coli detection," Journal of Biophotonics, vol. 24, 2017.

[34] K. Dandapat, S.M. Tripathi, Y.Chinifooroshan, W.J. Bock, and P. Mikulic, "temperature-insensitive bio-sensor based on long-period fiber gratings for accurate detection of E. coli bacteria in water," Optics Letters, vol. 41, no. 18, pp. 4198-4201, 2016.

[35] L. Chen, Y.K. Leng, B. Liu, J. Liu, and Q. Wu, "Ultrahigh-sensitivity label-free optical fiber biosensor based on a tapered singlemode-no core-singlemode coupler for Staphylococcus aureus detection," Sensors and Actuators B: Chemical, vol. 320, no. 1, pp. 128283, 2020.

[36] Y.C. Liao, B. Liu, J. Liu, S.P. Wan, X.D. He, J. Yuan, X. Fan, and Q. Wu, "High Temperature (Up to 950 °C) Sensor Based on Micro Taper In-Line Fiber Mach–Zehnder Interferometer," Appl. Sci, vol. 9, pp. 2394, 2019.

[37] H. Luo, Q. Sun, X. Li, Z. Yan, Y. Li, D. Liu, and L. Zhang, "Refractive index sensitivity characteristics near the dispersion turning point of the multimode microfiber-based Mach–Zehnder interferometer," Optics Letters, vol. 40, no. 21, pp. 5042-5, 2015.

[38] N. Duan, S. Wu, C. Zhu, X. Ma, Z. Wang, Y. Yu and Y. Jiang, "Dual-color upconversion fluorescence and aptamer-functionalized magnetic nanoparticles-based bioassay for the simultaneous detection of Salmonella Typhimurium and Staphylococcus aureus," Analytica Chimica Acta, vol. 723, no. 8, pp. 1-6, 2012.

[39] B. E. F. de Ávila, M. Pedrero, S. Campuzano, V. Escamilla-Gómez and J. M. Pingarrón, "Sensitive and rapid amperometric magnetoimmunosensor for the determination of Staphylococcus aureus," Analytical & Bioanalytical Chemistry, vol. 403, no. 4, pp. 917-925, 2012.

[40] N. Tawil, F. Mouawad, S. Lévesque, E. Sacher, R. Mandeville and M. Meunier, "The differential detection of methicillin-resistant, methicillin-susceptible and borderline oxacillin-resistant Staphylococcus aureus by surface plasmon resonance," Biosensors & Bioelectronics, vol. 49, pp. 334-340, 2013.

[41] J. Yuan, S. Wu, N. Duan, X. Ma, Y. Xia, J. Chen, Z. Ding and Z. Wang, "A sensitive gold nanoparticle-based colorimetric aptasensor for Staphylococcus aureus," Talanta, vol.127, pp. 163-168, 2014.

[42] R. Hernández, C. Vallés, A. M. Benito, W. K. Maser, F. X. Rius and J. Riu, "Graphene-based potentiometric biosensor for the immediate detection of living bacteria," Biosensors & Bioelectronics, vol. 54, pp. 553-557, 2014.

[43] J. F. Wang, X. Z. Wu, C. W. Wang, N. S. Shao, P. Dong, R. Xiao and S. Q. Wang, "Magnetically Assisted Surface-Enhanced Raman Spectroscopy for the Detection of Staphylococcus aureus Based on Aptamer Recognition," ACS Applied Materials & Interfaces, vol. 7, no. 37, pp. 20919-20929, 2015.

[44] A. Abbaspour, F. Norouz-Sarvestani, A. Noori and N. Soltani, "Aptamer-conjugated silver nanoparticles for electrochemical dual-aptamer-based sandwich detection of staphylococcus aureus," Biosensors & Bioelectronics, vol. 68, pp. 149-155, 2015.

[45] H. Ghali, H. Chibli, J. L. Nadeau, P. Bianucci and Y. Peter, "Real-Time Detection of Staphylococcus Aureus Using Whispering Gallery Mode Optical Microdisks," Biosensors, vol. 6, no. 2, pp. 20, 2016.

[46] G. A. R. Y. Suaifan, S. Alhogail and M. Zourob, "Rapid and low-cost biosensor for the detection of Staphylococcus aureus - ScienceDirect," Biosensors and Bioelectronics, vol. 90, pp. 230-237, 2016.

[47] F. Yan, T.L. Chan, T.C. Liu, D. Wu, and H. Du, "Label-free detection of Staphylococcus aureus bacteria using long-period fiber gratings with functional polyelectrolyte coatings," Biosens. Bioelectron, vol. 133, pp. 147－153, 2019.

[48] N. Bhardwaj, S. Kumar, D. Bhatt, S.K. Tuteja, Kim, Ki-Hyun, and A. Deep, "Highly sensitive optical biosensing of: staphylococcus aureus with an antibody/metal-organic framework bioconjugate," Anal. Methods, vol. 11, pp. 917－923, 2019.

Hou-Chang Li is a graduate student with the School of Measuring and Optical Engineering, Nanchang Hangkong University. His research interest is fiber optic sensing.

Yuan-Kui Leng received his bachelor's degree in 2010 on materials science from Zhejiang University. He obtained his PhD degree on materials science from Shanghai Jiao Tong University in 2017. Thereafter, he joined in School of Food Science & Technology, Nanchang University, and now he is focusing on the development of biosensors based on nanomaterials.

Yun-Cheng Liao is a graduate student with the School of Measuring and Optical Engineering, Nanchang Hangkong University. Her research interest is fiber optic sensing.

Bin Liu received his B.S. and Ph.D. degree from Sun Yat-sen University, China. Dr. Liu is an associate Professor with Key Laboratory of Nondestructive Test (Ministry of Education) of Nanchang Hangkong University, China. His main research interest is fiber optic sensing.

Wei Luo is a graduate student with the School of Measuring and Optical Engineering, Nanchang Hangkong University. Her research interest is fiber optic sensing.

Juan Liu received her Ph.D. degree from Beijing Normal University, China. She is a lecture with Key Laboratory of Nondestructive Test (Ministry of Education) of Nanchang Hangkong University, China. Her main research interest is fiber optic sensing.

Jiulin Shi received her Ph.D. degree from Huazhong University of Science and Technology, China. He is Professor of Key Laboratory of Opto-Electronic Information Science and Technology of Jiangxi Province, Nanchang Hangkong University. Her main research interest is multi-spectrum detection.

Jinhui Yuan received the Ph.D. degree in physical electronics from Beijing University of Posts and Telecommunications (BUPT), Beijing, China, in 2011. He is currently a Professor at the Department of computer and communication engineering, University of Science and Technology Beijing (USTB). He was selected as a Hong Kong Scholar at the Photonics Research Centre, Department of Electronic and Information Engineering, The Hong Kong Polytechnic University, in 2013. His current research interests include photonic crystal fibers, silicon waveguide, and optical fiber devices. He is the Senior Members of the IEEE and OSA. He has published over 200 papers in the academic journals and conferences.

Hengyi Xu received his BSc degree in Hebei University of Science and Technology in 2004, and obtained his MSc and PhD degree in the School of Food Science, Nanchang University in 2007 and 2010, respectively. He is presently a full professor in the State Key Laboratory of Food Science and Technology in Nanchang University, China. His main research interests are applications of nanomaterials for foodborne pathogen detection and biomedical diagnosis. He has published more than 50 peer-reviewed papers in international journals.

Yonghua Xiong received his BSc degree and PhD degree in the School of FoodScience, Nanchang University in 1992 and 2004, respectively. He is presently a pro-fessor in the State Key Laboratory of Food Science and Technology in NanchangUniversity, China. His research interests include ultrasensitive detection of myco-toxins using nanoparticle-based sesors.

Xing-Dao He was born in Jingan, China, in 1963. He received the Ph.D. degree in optics from Beijing Normal University, Beijing, China, in 2005. He is currently a Professor with the Key Laboratory of Nondestructive Test (Ministry of Education), Nanchang Hangkong University, China. His current research interests include light scattering spectroscopy, optical holography, and information processing.

Qiang Wu received the B.S. and Ph.D. degrees from Beijing Normal University and Beijing University of Posts and Telecommunications, Beijing, China, in 1996 and 2004, respectively. From 2004 to 2006, he worked as a Senior Research Associate in City University of Hong Kong. From 2006 to 2008, he took up a research associate post in Heriot-Watt University, Edinburgh, U.K. From 2008 to 2014, he worked as a Stokes Lecturer at Photonics Research Centre, Dublin Institute of Technology, Ireland. He is an Associate Professor / Reader with Faculty of Engineering and Environment, Northumbria University, Newcastle Upon Tyne, United Kingdom. His research interests include optical fiber interferometers for novel fiber optical couplers and sensors, nanofiber, microsphere sensors for bio-chemical sensing, the design and fabrication of fiber Bragg grating devices and their applications for sensing, nonlinear fibre optics, surface plasmon resonant and surface acoustic wave sensors. He has over 200 publications in the area of photonics and holds 3 invention patents. He is an Editorial Board Member of Scientific Reports, an Associate Editor for IEEE Sensors Journal and an Academic Editor for Journal of Sensors.